

Compact and integrated TM-pass waveguide polarizer

Chyong-Hua Chen, Lin Pang, Chia-Ho Tsai, Uriel Levy and Yeshaiah Fainman

*Department of Electrical and Computer Engineering, University of California, San Diego
9500 Gilman Dr. La Jolla, CA 92093-0408, USA
phone: 858-534-7208
chyong@ece.ucsd.edu*

Abstract: A novel integrated TM-pass waveguide polarizer with a subwavelength-wide slot is introduced and theoretically analyzed. With a proper design of the slot, the waveguide can be used as a single polarization waveguide to guide only TM polarization modes of the light signal. With 26 μm length of this TM-pass polarizer, our computer simulations predict the insertion loss of 0.54 dB for the TM polarization mode with the extinction ratio of 20.3 dB at the wavelength of 1.55 μm .

©2005 Optical Society of America

OCIS codes: (130.3120) Integrated optics devices, (230.5440) Polarization-sensitive devices, (230.7370) Waveguides.

References and links

1. E. M. Garmire and H. Stoll, "Propagation losses in metal-film-substrate optical waveguide," *IEEE J. Quantum Electron.* **8**, 763-6 (1972).
2. W. Johnstone, G. Stewart, T. Hart, and B. Culshaw, "Surface plasmon polaritons in thin metal films and their role in fiber optic polarizing devices," *J. Lightwave Technol.* **8**, 538-44 (1990).
3. T. Nakano, K. Baba, and M. Miyagi, "Insertion loss and extinction ratio of a surface plasmon-polariton polarizer: theoretical analysis," *J. Opt. Soc. Am. B* **11**, 2030-5 (1994).
4. C-H Chen, L. Wang, "Design of Finite-length metal-clad optical waveguide polarizer," *IEEE J. Quantum Electron.* **34**, 1089-97 (1998).
5. O. Watanabe, M. Tsuchimori, A. Okada, and H. Ito, "Mode selective polymer channel waveguide defined by the photoinduced change in birefringence," *Appl. Phys. Lett.* **71**, 750-2 (1997)
6. A. Morand, C. Sanchez-Perez, P. Benech, S. Tedjini, and D. Bosc, "Integrated optical waveguide polarizer on glass with a birefringent polymer overlay," *IEEE Photonics Technol. Lett.* **10**, 1599-601 (1998)
7. M. J. B.J. Wang, S. Schablitsky, Z. Yu, W. Wu, and S. Y. Chou, "Fabrication of a new broadband waveguide polarizer with a double-layer 190 nm period metal-gratings using nanoimprint lithography," *J. Bac. Sci. Technol. B.* **17**, 2957-60 (1999)
8. M.A. Khan and H.A. Jamid, "Analysis of TM-pass reflection mode optical polarizer using method of lines," in *Proceedings of the 2003 10th IEEE International Conference on Electronics, Circuits, and Systems* (Institute of Electrical and Electronics Engineers, New York, 2003). IEEE. Part Vol.2, pp. 555-8.
9. M. J. Bloemer, and J. W. Haus, "Broadband waveguide polarizers based on the anisotropic optical constants of nanocomposite films," *J. Lightwave Technol.* **14**, 1534-1540 (1996)
10. S.K. Kim, K. Geary, D. H. Chang, H.R. Fetterman, H. Zhang, C. Zhang, C. Wang, and W.H. Steier, "TM-pass polymer modulators with poling-induced waveguides and self-aligned electrodes," *Electron. Lett.* **39**, 721-2 (2003).
11. K. Baka, T. Iden, and M. Miyagi, "TM-pass glass waveguide polarizer with periodic multilayer cladding overlaid with isotropic dielectric media," *Electron. Lett.* **36**, 1461-2 (2000).
12. S.S. Lee, S. Garner, A. Chen, V. Chuyanov, W. H. Steier, S. W. Ahn, and S-Y Shin, "TM-pass polarizer based on a photobleaching-induced waveguide in polymers," *IEEE Photonics Technol. Lett.* **10**, 836-8 (1998)
13. H.A. Haus, W.P. Huang, and A.W. Snyder, "Coupled-mode formulations," *Opt. Lett.* **14**, 1222-4 (1989)
14. P. L. Liu, and B. J. Lin, "Study of form birefringence in waveguide devices using the semivectorial beam propagation method," *IEEE Photonics Technol. Lett.* **3**, 913-15 (1991)
15. V. R. Almeida, Qianfan Xu, C. A. Barrios and M. Lipson, "Guiding and confining light in void nanostructure," *Opt. Lett.* **29**, 1209-11 (2004)

16. A. Taflove, *Computational Electrodynamics: the Finite-Difference Time-Domain Method* (Artech House, Boston, 1995).
 17. K. Kawano and T. Kitoh, *Introduction to Optical Waveguide Analysis: Solving Maxwell's Equations and the Schrödinger Equation* (J. Wiley, New York, 2001).
 18. H. Nishihara, M. Haruna, and T. Suhara, *Optical Integrated Circuits* (McGraw-Hill, New York, 1989).
-

1. Introduction

Optical waveguide polarizers are essential components in integrated photonics, especially for devices and systems operating with a single polarization (SP) such as fiber-optic gyroscopes, electro-optic switching arrays, coherent optical communication modules and more. The functionality of optical waveguide polarizers is to allow only one polarization state (transverse electric (TE) or transverse magnetic (TM)) to propagate while the other polarization state is eliminated. A good polarizer is characterized by low insertion loss and high extinction ratio. Many types of waveguide polarizers have been realized over the years, including, for example, metal-clad waveguides [1-4] and birefringence waveguides [5,6], but only few of them are TM-pass types. One class of such polarizers is based on using a metal-cladding layer with either a grating [7,8] or a nanocomposite structure [9] to absorb the propagating TE polarization wave. However, the propagation loss of these devices is relatively high. A different concept is using a polarization splitter structure such as a directional coupler to split TE and TM modes into horizontal or vertical integrated waveguides [10], but for either of the cases complex and specific structures need to be used. Devices based on deposition of birefringent materials or form birefringent multilayers have been proposed as well, where TE polarization is eliminated due to different TE and TM cutoff wavelengths [11,12]; but unfortunately relatively long distance (usually several millimeters) is needed to achieve high extinction ratio.

It is well known that most of waveguide devices are polarization dependent due to the different boundary conditions for each polarization [13,14]. Typically, TE and TM modes propagate with slightly different propagation constants. The birefringence increases as the structure has abrupt index change and geometrical variations, e.g. slot waveguides [15]. These types of birefringent waveguides have been demonstrated for mostly air guiding of the TE-like mode. In this paper, we propose a novel TM-pass waveguide polarizer based on geometry-induced birefringence. Our device is based on introducing a slot into the waveguide, operating as a directional coupler that produces high birefringence. By proper design, the waveguide confines only TM modes, i.e. a SP waveguide is achieved. With integration of Y-branch mode-converted waveguides, a high extinction ratio and low loss TM-pass polarizer is realized. The proposed device is based on a GaAs ridge waveguide on top of an AIAs layer, although the concept can be easily applied to other material systems, e.g. silicon on insulator (SOI) and polymer waveguides. By using three-dimensional (3-D) semivectorial finite difference time domain (FDTD) method [16], a numerical study of this polarizer is carried out. The simulation results indicate that the extinction ratio of 20.3 dB and the insertion loss of 0.54 dB can be obtained with a device length of 26 μm at the wavelength of 1.55 μm .

2. Design of a TM-pass waveguide polarizer

The proposed device is composed of identical input and output waveguides and a TM-pass polarizer in between. The device consists of GaAs ($n=3.374$) as a guiding layer and AIAs ($n=2.95$) as a substrate layer. The input and the output sections are designed as single mode ridge waveguides operating at 1.55 μm wavelength. Let the width of the waveguide be $W=1 \mu\text{m}$ and its height be $H=0.5 \mu\text{m}$. The effective indices of TE_{00} and TM_{00} modes calculated by

semivectorial finite difference (FD) method with Dirichlet boundary conditions [17] are 3.119 and 3.085, respectively.

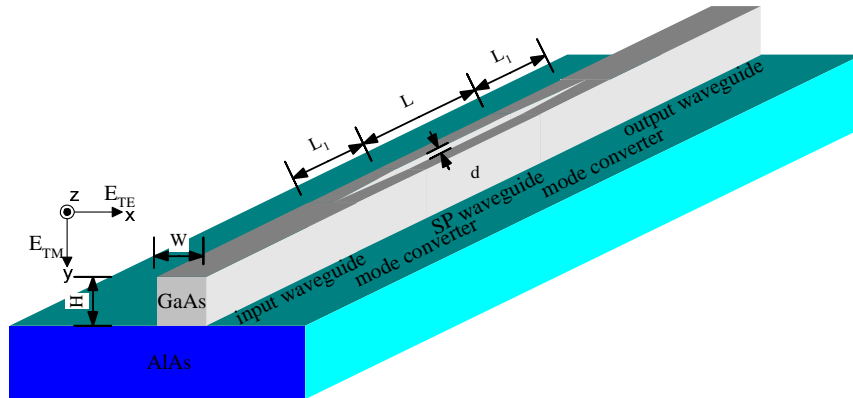


Fig. 1. The schematic structure of the TM-pass polarizer. The input and output waveguides are ridge waveguides with width W and height H . A TM-pass SP waveguide is a ridge waveguide with the same size of input and output. A slot filled with air is centered at the SP waveguide with width d and length L . Y-branch mode-conversion waveguides are between input/output and SP waveguides with the length of L_1 .

The TM-pass polarizer consists of a TM-like SP waveguide sandwiched between two identical mode-converters. A schematic drawing of the proposed design is shown in Fig. 1 with L_1 being the length of the mode converter, L being the length of the TM-like SP waveguide and d being the distance between the two parallel waveguides.

First, we investigate the polarization dependence of the SP waveguide shown in Fig. 1. The width of each ridge waveguide is w_1 . Its height is H , same as the input and output (I/O) waveguides, i.e. $0.5 \mu\text{m}$. The separation between the two waveguides is d , and the total width is $d+2w_1=W$. The cross-section of the proposed SP waveguide structure (onset) and effective indices of the lowest TE-like and TM-like modes of this waveguide versus d are shown in Fig. 2. The results clearly indicate that effective indices for the two polarization modes decrease as d increases. However, the effective index of the TE-like mode (dashed line) decreases much faster than that of the TM-like mode (solid line). No guided mode for the TE polarization is supported as $d > 0.02 \mu\text{m}$, while a guided TM-like mode is sustained as long as $d < 0.14 \mu\text{m}$. Therefore, if the separation distance d is between 0.02 and $0.14 \mu\text{m}$, a TM-like SP waveguide can be realized.

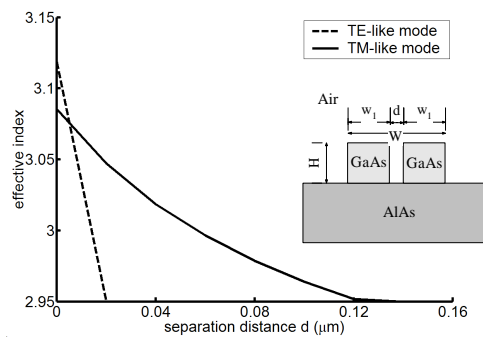


Fig. 2. Effective indices for the lowest TE-like (dashed line) and TM-like (solid line) modes of the SP waveguide versus different separation distance d . The inset shows the cross-section of the simulated SP waveguide.

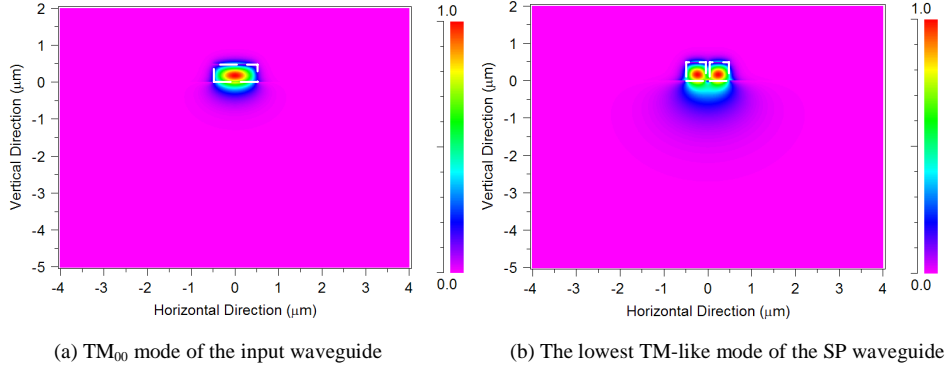


Fig. 3. E_y field profiles of the fundamental TM modes of the input waveguide (left) and the SP waveguide with $d=0.1 \mu\text{m}$ (right). The white dashed line shows the cross section of waveguides.

The field distributions of the fundamental TM modes for the input and the SP waveguides with $d=0.1 \mu\text{m}$ are shown in Fig. 3. Since the TM field is localized within the high-index region, there is a significant mode mismatch between the I/O waveguides and the SP waveguide, giving rise to substantial insertion loss. The coupling efficiency from the input waveguide to the SP waveguide with $d=0.1 \mu\text{m}$ was found to be 0.86, calculated by the following overlap integral [18] with $E_{in}(x,y)$ and $E_{out}(x,y)$ denoting the mode profiles of the input and the SP waveguides, respectively:

$$\eta = \frac{\left| \iint E_{in}(x,y) E_{out}(x,y) dx dy \right|^2}{\iint |E_{in}(x,y)|^2 dx dy \iint |E_{out}(x,y)|^2 dx dy} \quad (1)$$

The coupling loss due to mode mismatch at the interface of the input and the SP waveguides given by $10\log_{10}(\eta)$ is -0.67 dB. In order to mitigate the coupling loss, we introduce mode conversion sections between the I/O and the SP waveguides. The mode converter allows an adiabatic mode transition from the I/O waveguide sections to the SP waveguide.

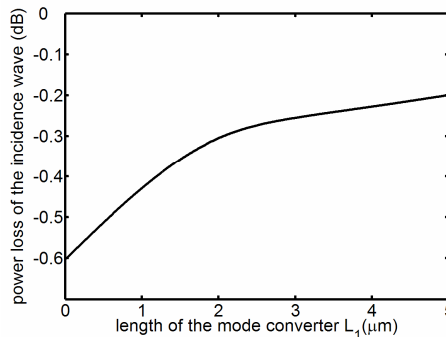


Fig. 4. Power loss of the TM_{00} mode incidence wave with variations of the length of the Y-branch waveguide L_1 .

We use an inner symmetric Y-branch waveguide with length L_1 as a mode converter shown in Fig. 1. In Fig. 4, we show the effects of the variations of L_1 on the power loss of the incidence wave propagating along the structure consisting of an input waveguide, a mode converter with length $L_1 \mu\text{m}$ and the SP waveguide with $d=0.1 \mu\text{m}$ and $L=10 \mu\text{m}$. The calculated results are obtained by using 3-D FDTD method with the TM_{00} mode of the input waveguide as the input signal. One can see that the power loss diminishes as L_1 increases. As $L_1=0$, the power loss is -0.61 dB, slightly smaller than the value predicted by the overlap integral. This is probably because the radiation modes excited by the incidence wave do not

vanish entirely within 10 μm length of the SP waveguide. With $L_1 > 3 \mu\text{m}$, the mode conversion loss is less than -0.25 dB , which is acceptable for telecommunication applications.

Figures 5(a) and 5(b) show the calculated propagation behaviors in the waveguide polarizer with $L_1 = 3 \mu\text{m}$, $d = 0.1 \mu\text{m}$ and $L = 20 \mu\text{m}$ for TE and TM polarizations, respectively. The results are obtained using FDTD with the incidence wave at the input waveguide being the fundamental mode for each polarization. As expected, the guided TE-like mode is not supported in the SP waveguide, and thus the TE_{00} mode leaks into the substrate as it propagates through the polarizer. Contrarily, the TM_{00} mode is well confined in the SP waveguide structure without observable decay of the field power. The overall loss is minimized by the implementation of the mode converter.

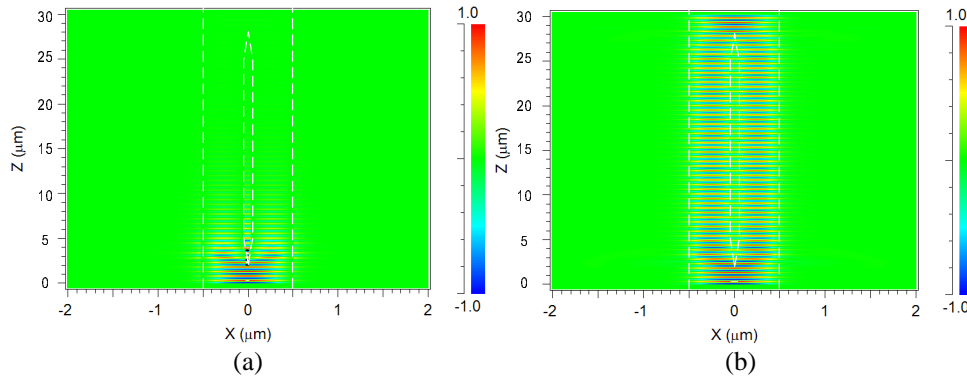


Fig. 5. Field distributions of the incidence waves with TE (left) and TM (right) polarizations propagating in the waveguide polarizer.

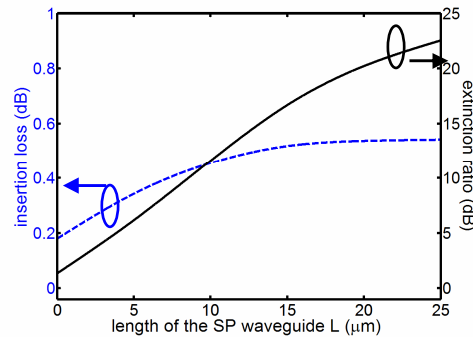


Fig. 6. Performance of the proposed TM polarizer with different length of the SP waveguide L . The dashed line is the insertion loss of the whole device and the solid line is the extinction ratio.

Figure 6 shows the calculated insertion loss of the TM polarization and the extinction ratio of the waveguide polarizer as the function of the SP waveguide length L with $L_1 = 3 \mu\text{m}$ and $d = 0.1 \mu\text{m}$. Here, the extinction ratio of a polarizer is defined as the power ratio of TM_{00} and TE_{00} modes in the output waveguide, i.e. $10\log_{10}(P_{\text{TM}_{00}}/P_{\text{TE}_{00}})$, where $P_{\text{TM}_{00}}$ and $P_{\text{TE}_{00}}$ are the power of TM_{00} and TE_{00} modes in the output waveguide. The insertion loss is defined as the total power loss of the TM_{00} mode in the output waveguide, i.e., $-10\log_{10}(P_{\text{TM}_{00}})$. For the TE polarization, the power loss increases with L and becomes larger than 20 dB at $L > 18.7 \mu\text{m}$. On the other hand, for the TM polarization, the power loss of about 0.54 dB is almost invariant with $L > 15 \mu\text{m}$, roughly twice the coupling loss from the mode converter with $L_1 = 3 \mu\text{m}$, since the TM-like mode is guided by the SP waveguide structure (scattering loss due to waveguide roughness was neglected due to the short length of the device). As $L = 20 \mu\text{m}$, the device possesses the extinction ratio of 20.3 dB and the insertion loss of 0.54 dB .

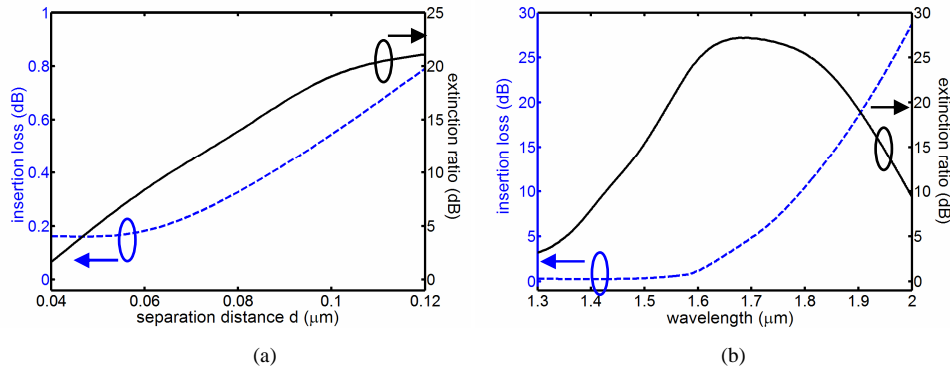


Fig. 7. (a) Insertion loss and extinction ratio of the polarizer with variations of the separation distance d . (b) Insertion loss and extinction ratio as a function of wavelength.

Figure 7(a) shows the effects of the variations of the separation distance d on the insertion loss and the extinction ratio of the polarizer with $L_1=3 \mu\text{m}$ and $L=20 \mu\text{m}$. We see that both the extinction ratio and the insertion loss grow with the increase of d . The extinction ratio is increasing with d because the propagation loss of the TE_{00} mode in the SP waveguide is increasing, while the propagation loss for the TM_{00} mode is negligible over the range of 20 μm . On the other hand, mode mismatch between the input and the SP waveguides becomes larger with the increase of d , and consequently the power loss for the TM polarization, predominately resulting from the coupling loss, also increases. This can be compensated by using a longer mode converter (larger value of L_1). The corresponding cutoff wavelengths for the lowest TE-like and TM-like modes of the SP waveguide with $d=0.1 \mu\text{m}$ are 1.32 and 1.61 μm respectively, defining the wavelength region of operation for the proposed device. The wavelength dependency of a typical device with $L_1=3 \mu\text{m}$, $d=0.1 \mu\text{m}$ and $L=20 \mu\text{m}$ is shown in Fig. 7(b), which is calculated by using 3-D FDTD with TE_{00} and TM_{00} modes as the incidence waves. One can easily notice that the insertion loss remains approximately constant for wavelength shorter than 1.61 μm . The extinction ratio shows an optimum around 1.68 μm . This is because the power loss of the TE_{00} mode decreases significantly for shorter wavelengths, while the power loss of the TM_{00} mode increases for wavelength larger than 1.61 μm .

4. Conclusions

A TM-pass waveguide polarizer is proposed and analyzed. The device consists of a coupler waveguide section supporting only TM-like modes, and a Y-branch section allowing an adiabatic mode conversion between the input/output waveguides and the SP ridge waveguide. The device is optimized using 3-D semivectorial FDTD method. With a length 20 μm of the SP waveguide and two 3 μm -long Y-branch waveguides, an extinction ratio of 20.3 dB is obtained with the insertion loss in the order of 0.5 dB. Higher extinction ratio can be achieved either by increasing the length of the SP waveguide or by increasing the separation distance with only a slight increase of the insertion loss. In addition, the insertion loss of the device could be reduced either by increasing the length of the mode converter or by reducing the separation distance of the two waveguides.

Acknowledgments

The authors acknowledge the support of the Defense Advanced Research Projects Agency, the National Science Foundation, and the U.S. Air Force Office of Scientific Research.